




Article

# Comparative Proteomic Profiling of Marine and Freshwater *Synechocystis* Strains Using Liquid Chromatography-Tandem Mass Spectrometry

Dami Kwon <sup>1,†</sup>, Jong-Moon Park <sup>1,2,†</sup> , Van-An Duong <sup>1,†</sup> , Seong-Joo Hong <sup>3</sup>,  
Byung-Kwan Cho <sup>4</sup>, Choul-Gyun Lee <sup>3</sup>, Hyung-Kyoon Choi <sup>5</sup>, Dong-Myung Kim <sup>6</sup>  
and Hookeun Lee <sup>1,\*</sup> 

<sup>1</sup> College of Pharmacy, Gachon University, Incheon 21936, Korea; kan\_u@naver.com (D.K.); bio4647@naver.com (J.-M.P.); anduong@gachon.ac.kr (V.-A.D.)

<sup>2</sup> Basilbiotech, Seoul 06621, Korea

<sup>3</sup> Department of Biological Engineering, Institute of Industrial Biotechnology, Inha University, Incheon 402-751, Korea; owlet77@gmail.com (S.-J.H.); leecg@inha.ac.kr (C.-G.L.)

<sup>4</sup> Department of Biological Sciences, Korea Advanced Institute of Science and Technology (KAIST), Daejeon 305-701, Korea; bkcho01@gmail.com

<sup>5</sup> College of Pharmacy, Chung-Ang University, Seoul 156-756, Korea; hykychoi@cau.ac.kr

<sup>6</sup> Department of Fine Chemical Engineering and Applied Chemistry, Chungnam National University, Daejeon 34134, Korea; dmkim@cnu.ac.kr

\* Correspondence: hkleee@gachon.ac.kr; Tel.: +82-32-820-4927

† These authors contributed equally to this work.

Received: 1 September 2020; Accepted: 9 October 2020; Published: 12 October 2020



**Abstract:** Freshwater *Synechocystis* sp. PCC 6803 has been considered to be a platform for the production of the next generation of biofuels and is used as a model organism in various fields. Various genomics, transcriptomics, metabolomics, and proteomics studies have been performed on this strain, whereas marine *Synechocystis* sp. PCC 7338 has not been widely studied despite its wide distribution. This study analyzed the proteome profiles of two *Synechocystis* strains using a liquid chromatography–tandem mass spectrometry-based bottom-up proteomic approach. Proteomic profiling of *Synechocystis* sp. PCC 7338 was performed for the first time with a data-dependent acquisition method, revealing 18,779 unique peptides and 1794 protein groups. A data-independent acquisition method was carried out for the comparative quantitation of *Synechocystis* sp. PCC 6803 and 7338. Among 2049 quantified proteins, 185 up- and 211 down-regulated proteins were defined in *Synechocystis* sp. PCC 7338. Some characteristics in the proteome of *Synechocystis* sp. PCC 7338 were revealed, such as its adaptation to living conditions, including the down-regulation of some photosynthesis proteins, the up-regulation of kdpB, and the use of osmolyte glycine as a substrate in C1 metabolism for the regulation of carbon flow. This study will facilitate further studies on *Synechocystis* 7338 to define in depth the proteomic differences between it and other *Synechocystis* strains.

**Keywords:** *Synechocystis* 6803; *Synechocystis* 7338; proteomics; global identification; LC-MS/MS; marine; freshwater; data-independent acquisition; photosynthesis

## 1. Introduction

Cyanobacteria, the only prokaryotes that perform oxygenic photosynthesis, have been considered as an attractive source for the direct production of chemicals and bioenergy from carbon dioxide (CO<sub>2</sub>) [1–5]. Various studies on cyanobacteria have been conducted to date, and *Synechocystis* species are frequently used as model organisms [6–8]. *Synechocystis* is widely distributed across the Earth,

with approximately 2000 species in about 150 genera. Cyanobacteria *Synechocystis* comprise the base of the food chain of the marine ecosystem [9]. *Synechocystis* has the potential to become a platform for biofuel production due to its fast growth, ability to fix CO<sub>2</sub>, and high lipid content [10–13]. A number of studies have been conducted on *Synechocystis* to investigate its photosynthesis, stress reaction and evolution processes [14,15]. One of the most used *Synechocystis* strains in recent studies is freshwater *Synechocystis* sp. PCC 6803 (hereafter, *Synechocystis* 6803) [16–18]. The gene functions and transformation mechanisms of *Synechocystis* have been studied at the genome level after the genome of *Synechocystis* 6803 was fully sequenced in 1996 [19]. It also produces various commodity chemicals such as ethanol, alkanes, fatty alcohol, fatty acids, ethylene, isoprene, and lactic acid [20–23]. Besides the freshwater strain, marine *Synechocystis* sp. PCC 7338 (hereafter, *Synechocystis* 7338) is also an alternative organism that has the potential to be used in various fields. Although it was first isolated in 1970, only a few studies have been performed on this marine strain [24]. Interest in producing various physiologically active substances derived from this marine cyanobacteria has emerged so far [25,26]. Recently, the metabolic and lipidomic profiling of *Synechocystis* 7338 has been carried out. Furthermore, a quantitative comparison between the freshwater and marine strains was performed, revealing that the diacylglyceryltrimethylhomoserine group existed only in the latter strain. The study revealed metabolic differences of the marine strain under long-term exposure to salinity [27].

A comparative proteomic study of *Synechocystis* 6803 and 7338 could enhance the understanding of the differences between the strains at the protein level. Previously, a comparative proteomic analysis of two strains of the same species was able to reveal their different biological behaviors and particular distinctions between them [28,29]. Proteomic research on cyanobacteria has been accompanied by the development of mass technology [30,31]. The combination of two-dimensional gel electrophoresis (2-DE) and liquid chromatography–tandem mass spectrometry (LC-MS/MS) has been used in various proteomic studies on *Synechocystis* 6803 [32–36] and has found up to several hundreds of proteins. A two-dimensional (2D) separation was used to increase protein identification to approximately 2000 [37]. A label-free LC-MS/MS proteomic approach identified 1736 proteins and quantified 812 proteins, which revealed global proteome changes of this species to an extreme copper environment [38]. Another quantitative proteomic study performed dimethylation labeling and 2D separation to determine the proteome and phosphoproteome changes in *Synechocystis* 6803 during resuscitation and identified 2461 proteins [39]. In a recent study, Baers and coworkers used tandem mass tags (TMT) 10-plex labeling and 2D separation to identify 2445 proteins and reveal distinct compartment organization in this species [40]. A similar strategy was conducted to determine the alterations in the proteomic expression of *Synechocystis* 6803 induced by the antibiotics sulfamethoxazole and tetracycline [41]. In addition, other studies performed shotgun bottom-up proteomic approaches for the identification and quantification of peptides and proteins in the freshwater strain. These studies utilized label-free quantification [42,43] and isobaric tags for relative and absolute quantitation (iTRAQ) [44–49]. Proteomic studies on *Synechocystis* 6803 have contributed to a better understanding of *Synechocystis* species, such as the critical roles of FtsH1/3 complex in acclimation to iron, phosphate, carbon, and nitrogen starvation in *Synechocystis* [50], the regulatory role of cytochrome cM in photomixotrophy [51], and changes in its proteome and phosphoproteome under photoautotrophic, mixotrophic, heterotrophic, dark, and nitrogen-deprived conditions [52]. However, there has been no available report on the proteomic analysis of *Synechocystis* 7338. Thus, in this study, we carried out comparative proteomic profiling of the marine and freshwater *Synechocystis* strains using the data-independent acquisition (DIA) method. The study aimed to investigate characteristic proteomic profiles of *Synechocystis* 7338. By comparing the protein expression differences between the freshwater and marine *Synechocystis*, the study deepened our understanding of the metabolic mechanisms of the marine strain.

## 2. Materials and Methods

### 2.1. Materials

*Synechocystis* 6803 and 7338 were purchased from Pasteur Culture Collection (Paris, France). Tris (2-carboxyethyl)phosphine (TCEP) was obtained from Thermo Fisher Scientific (Rockford, IL, USA). Iodoacetamide (IAA), formic acid (FA), trifluoroacetic acid (TFA), and trimethylamine (TEA) were supplied by Sigma-Aldrich (St. Louis, MO, USA). Trypsin was purchased from Promega (Madison, WI, USA). High-performance liquid chromatography (HPLC)-grade water and acetonitrile (ACN) were obtained from JT Baker (Phillipsburg, NJ, USA).

### 2.2. Culture Conditions

*Synechocystis* 6803 and 7338 were grown photoautotrophically at  $30 \mu\text{E m}^{-2} \text{s}^{-1}$  from fluorescent lamps (Dulux L 36W/954, Osram, Munich, Germany).  $\text{CO}_2$  was controlled at 2%, and the temperature was maintained at  $30 \pm 1 \text{ }^\circ\text{C}$ . *Synechocystis* 6803 was cultivated in a 1 L flask with 400 mL of blue-green medium (BG-11, Sigma-Aldrich),  $\text{K}_2\text{HPO}_4$  (30.5 mg/L),  $\text{Na}_2\text{CO}_3$  (20 mg/L), ammonium iron citrate (6 mg/L), and trace metal mix A5 with cobalt (1 mL/L, Sigma-Aldrich). *Synechocystis* 7338 was cultivated in a 0.5 L bubble column photobioreactor with 0.4 L artificial seawater nutrient medium (ASN-III), which consisted of NaCl (25 g/L),  $\text{MgCl}_2 \cdot 6\text{H}_2\text{O}$  (2 g/L),  $\text{MgSO}_4 \cdot 7\text{H}_2\text{O}$  (3.5 g/L),  $\text{CaCl}_2 \cdot 2\text{H}_2\text{O}$  (0.5 g/L), KCl (0.5 g/L),  $\text{NaNO}_3$  (0.75 g/L), citric acid (3 mg/L),  $\text{K}_2\text{HPO}_4 \cdot 3\text{H}_2\text{O}$  (20 mg/L), ethylenediaminetetraacetic acid (EDTA)- $\text{Na} \cdot 2\text{H}_2\text{O}$  (5 mg/L), ammonium iron citrate (3 mg/L), and trace metal mix A5 with cobalt (2 mL/L, Sigma-Aldrich). The initial cell density was 0.1 g/L in each flask. When the cells reached the mid-exponential phase of each strain (days 5 and 8 for *Synechocystis* 6803 and 7338, respectively), they were harvested using centrifugation, lyophilized, and stored at  $-80 \text{ }^\circ\text{C}$  until use [27]. The experiment was conducted in triplicate. Cells from three flasks per strain were pooled, and one final sample per strain was used for proteomic analysis.

### 2.3. Whole-Cell Protein Tryptic Digestion

Samples were thawed at  $4 \text{ }^\circ\text{C}$  prior to whole-cell protein tryptic digestion. Stabilizer T1 (Denator AB, Uppsala Science Park, Sweden) was used to apply an instantaneous high temperature ( $95 \text{ }^\circ\text{C}$ ) for heat stabilization to stop degradation [53]. For cell lysis, each sample was dispersed in 3 mL of lysis buffer (8 M urea, 0.1 M Tris-HCl, pH 8.5), and a focus sonication was conducted for 15 min at  $18 \text{ }^\circ\text{C}$  using Covaris S2 (Covaris, Woburn, MA, USA). Proteins were precipitated with acetone ( $-20 \text{ }^\circ\text{C}$ ) for 18 h. The samples were centrifuged at 4000 rpm and  $4 \text{ }^\circ\text{C}$  for 10 min using a Centrifuge 5810 R (Eppendorf, Hamburg, Germany) to collect the protein pellet. After evaporating the solvent at 1800 rpm for 3 h with the Speed-Vac (Bio-Rad, Hercules, CA, USA), the proteins were washed with acetone ( $-20 \text{ }^\circ\text{C}$ ) and then dissolved in the lysis buffer. After quantifying each sample with a Pierce BCA (bicinchoninic acid) Protein Assay kit (Thermo Fisher Scientific), the protein concentration was adjusted to 1 mg/150  $\mu\text{L}$  using lysis buffer. Proteins were reduced with 1.5  $\mu\text{L}$  of 500 mM TCEP (300 rpm,  $37 \text{ }^\circ\text{C}$ , 45 min) and alkylated with 4.5  $\mu\text{L}$  of 500 mM IAA in the dark (300 rpm,  $37 \text{ }^\circ\text{C}$ , 45 min) using a Thermomixer comfort (Eppendorf, Hamburg, Germany). Trypsin was added for digestion at an enzyme:protein ratio of 1:50 (w/w) (300 rpm,  $37 \text{ }^\circ\text{C}$ , 16 h). After the incubation, 0.1% formic acid (FA) was added to stop the action of trypsin. Samples were then stored at  $-20 \text{ }^\circ\text{C}$  until the desalting step. Sep-Pak Vac 1cc (50 mg) C18 cartridges (Waters Corporation, Milford, MA, USA) were used for desalting [54]. The solvent was evaporated at 1800 rpm for 3 h with the Speed-Vac. The sample was then dissolved in 0.1% FA, followed by centrifugation at  $12,000 \times g$  for about 1 min to remove any pellets.

### 2.4. High pH RP Fractionation

Peptide mixtures from each *Synechocystis* strain were subjected to high pH reversed-phase (RP) fractionation [55]. A series of 16 eluting solutions consisting of 0.1% TEA in an ACN:water mixture

was prepared. The amount of ACN was increased stepwise from 2.5% to 50% (v/v). The fractionation was performed using Sep-Pak<sup>®</sup> Vac 1 cc tC18 cartridges (Waters, Milford, MA, USA). The column conditioning steps were as follows: 1 mL of methanol, 1 mL of ACN (twice), and 1 mL of 0.1% TFA (twice). The sample was then loaded into the column, followed by 16 stepwise elution steps with increasing ACN levels. Sixteen fractions (numbered from 1 to 16) were pooled to obtain five final high pH RP fractions (1–6–11, 2–7–12, 3–8–13, 4–9–14, and 5–10–15–16) [56]. After drying with the Speed-Vac (1800 rpm, 3 h), the samples were dissolved in 0.1% FA for analysis.

### 2.5. Mass Spectrometric Acquisition

Dionex Ultimate 3000 nanoUPLC coupled with Q-Exactive<sup>™</sup> Hybrid Quadrupole-Orbitrap MS (Thermo Scientific, San Jose, CA, USA) was used for the analysis of peptides. An Acclaim<sup>™</sup> PepMap<sup>™</sup> 100 C18 nano-trap column (75  $\mu\text{m} \times 2 \text{ cm}$ , 3  $\mu\text{m}$  particles, 100  $\text{\AA}$  pores, Thermo Fisher Scientific) was used to load the sample with the help of 0.1% FA in water (solvent A) at a flow rate of 2.5  $\mu\text{L}/\text{min}$  for 5 min. The peptides were separated using an Acclaim<sup>™</sup> PepMap<sup>™</sup> C18 100A RSLC nano-column (75  $\mu\text{m} \times 50 \text{ cm}$ , 2  $\mu\text{m}$  particles, 100  $\text{\AA}$  pores, Thermo Fisher Scientific) at a flow rate of 300 nL/min. The mobile phase solvent consisted of solvent A and 0.1% FA in ACN (solvent B). A 185 min gradient set up for solvent B was used as follows: 4% (0–14 min), 4–40% (14–155 min), 40–96% (155–157 min), 96% (157–169 min), 96–4% B (169–170 min), and 4% (170–185 min). The nano-electrospray ionization source was operated under the positive mode. MS parameters included the following: spray voltage, 2.0 kV; capillary temperature, 320  $^{\circ}\text{C}$ ; isolation width,  $\pm 2 m/z$ ; scan range 400–2000  $m/z$ ; resolution in full-MS scans, 70,000; resolution in MS/MS scans at 200  $m/z$ , 17,500; and dynamic exclusion, 20 s. Precursor ions were isolated in the quadrupole and fragmented via the higher-energy collisional dissociation with 27% normalized collisional energy. In the data-dependent acquisition (DDA) method, samples obtained from the high pH RP fractionation (five fractions per each *Synechocystis* strain) were analyzed, and the top 10 precursor ions with the highest intensity were selected for fragmentation. In the DIA method, the proteome digest of one biological replicate for each *Synechocystis* strain was analyzed. Each sample was analyzed four times for technical replicates. Twenty non-overlapping 20  $m/z$ -wide windows between 500 and 900  $m/z$  were set for the analysis.

### 2.6. Mass Spectrometric Data Analysis

The proteomics data were deposited with the ProteomeXchange Consortium via the PRIDE partner repository [57], with the dataset identifier PXD019340. For the identification, raw MS/MS files of 10 analyses in DDA MS were converted to mzXML format with MSConvert followed by analysis with Comet (Version 2018012) [58]. The MS/MS spectra were searched against the *Synechocystis* 6803 proteome database (a Uniprot/Swissprot fasta file of 3507 reviewed proteins, downloaded on 13 November 2017). Identification settings were as follows: maximum missed cleavage, 2; precursor mass tolerance, 10 ppm; fragment mass tolerance, 0.02 Da; static modification, carbamidomethylation of cysteine (+57.012 Da); variable modifications, oxidation of methionine (+15.995 Da) and carbamylation of protein N-term (+43.006 Da). The files obtained from the Comet search were imported into the Trans-Proteomic Pipeline (TPP) [59]. PeptideProphet [60] and ProteinProphet [61] were performed with a false discovery rate (FDR) of  $\leq 1\%$ . Only proteins identified with at least two peptides were selected. Decoys and duplicates in identified data were removed.

DDA data were also used to build a library for DIA data analysis using Skyline (ver. 4.2.0), which is open-source software [62]. The cut-off score was fixed at 0.99. Acquisition method settings were as follows: start  $m/z$ , 500; end  $m/z$ , 900; window width, 20  $m/z$ ; configured transition settings and configured full-scan setting were the same as MS settings; precursor charge, 1–4; ion charge, 1–2; ion types, y, b, p; ion match tolerance, 0.05  $m/z$ ; number of product ions picked, 5; maximum missed cleavages, 2; and minimum number of peptides per protein, 2 [63]. The fasta file from Uniprot of *Synechocystis* 6803 was input as a database. After analysis, the obtained data were processed with MSstats (ver. 3.13.6) [64]. Quantile normalization was applied. Student's t-test was used and the

$p$ -value was corrected using Benjamini–Hochberg correction. DEPs were identified with a  $|\log_2FC|$  of  $\geq 1$  (fold change) and an adjusted  $p$ -value of  $\leq 0.05$ .

### 2.7. Bioinformatics Analysis

Gene ontology (GO) analysis of DEPs was performed using GO enrichment analysis provided by the Genontology Consortium (<http://geneontology.org>) [65]. Classification using Panther included biological processes, cellular components, and molecular functions. Kyoto Encyclopedia of Genes and Genomes (KEGG) metabolic pathways with the KEGG Mapper tool were also identified [66]. Protein–protein interactions were analyzed using String [67] with the database of *Synechocystis* 6803.

## 3. Results and Discussion

### 3.1. Data-Dependent Acquisition (DDA) for Proteomic Profiling of *Synechocystis* 6803 and 7338

DDA is used for global proteomic profiling and comparative proteomics [68]. In this study, a DDA method was first performed to identify peptides and proteins in two *Synechocystis* strains as well as to build a spectrum library for the DIA analysis, whereas a DIA method was carried out for protein quantification and the comparison of protein abundance between two strains. To increase peptide and protein identification in DDA, a chromatographic separation following the pre-fractionation of high pH reverse-phase (RP) fractionation and low pH RP LC was utilized since it allows the deep profiling of the proteomes and its effectiveness had been previously reported [69,70]. In this study, the global proteomic profiling of *Synechocystis* 7338 was conducted for the first time, whereas *Synechocystis* 6803 was used as a reference. Proteome digests of *Synechocystis* 6803 and 7338 were simultaneously fractionated into five fractions for each sample followed by LC-MS/MS analysis with a DDA method. The proteomes of *Synechocystis* 6803 and 7338 were searched against a database of *Synechocystis* 6803 using TPP since the RNA sequencing of *Synechocystis* 7338 has not yet been published. After an MS/MS search with Comet, PeptideProphet and ProteinProphet were used for peptide and protein identification, respectively.

The lists of peptides identified with PeptideProphet and protein groups identified with ProteinProphet at an FDR of  $\leq 0.01$  are presented in Tables S1 and S2, respectively. Figure 1 shows the results of proteomic profiling using the 2D-LC system. First, as presented in Figure 1a, the numbers of MS/MS spectra acquired in each run were similar among 10 fractions. Each fraction (MS/MS time  $\sim 185$ -min) resulted in approximately 64,000 acquired MS/MS spectra, equivalent to 320,000 MS/MS spectra per sample. However, the number of assigned MS/MS spectra in *Synechocystis* 6803 was higher than that of *Synechocystis* 7338 ( $21,732 \pm 1383$  vs.  $15,214 \pm 1178$ ). In addition, the numbers of unique peptide IDs in *Synechocystis* 6803 and 7338 were  $10,763 \pm 1258$  and  $7658 \pm 667$ , respectively. Thus, the numbers of assigned MS/MS spectra and unique peptide IDs in *Synechocystis* 6803 were about 1.4-fold higher than those in *Synechocystis* 7338. It is obvious that, in each strain, the numbers of assigned MS/MS spectra and unique peptide IDs were similar among the five fractions, which indicates the even distribution of peptides following high pH RP fractionation. Furthermore, when using ProteinProphet to identify protein groups in each fraction of two samples, the numbers were similar among fractions (1326, 1468, 1446, 1346, and 1433 for *Synechocystis* 6803; 1013, 1078, 1090, 1031, and 1174 for *Synechocystis* 7338). Figure 1b presents the cumulative numbers of identified peptides and protein groups (single hit included) against the number of fractions. The number of peptides increased gradually with the number of fractions for both samples. However, the number of protein groups increased slowly after two fractions as a result of the redundancy of protein groups in the later fractions.



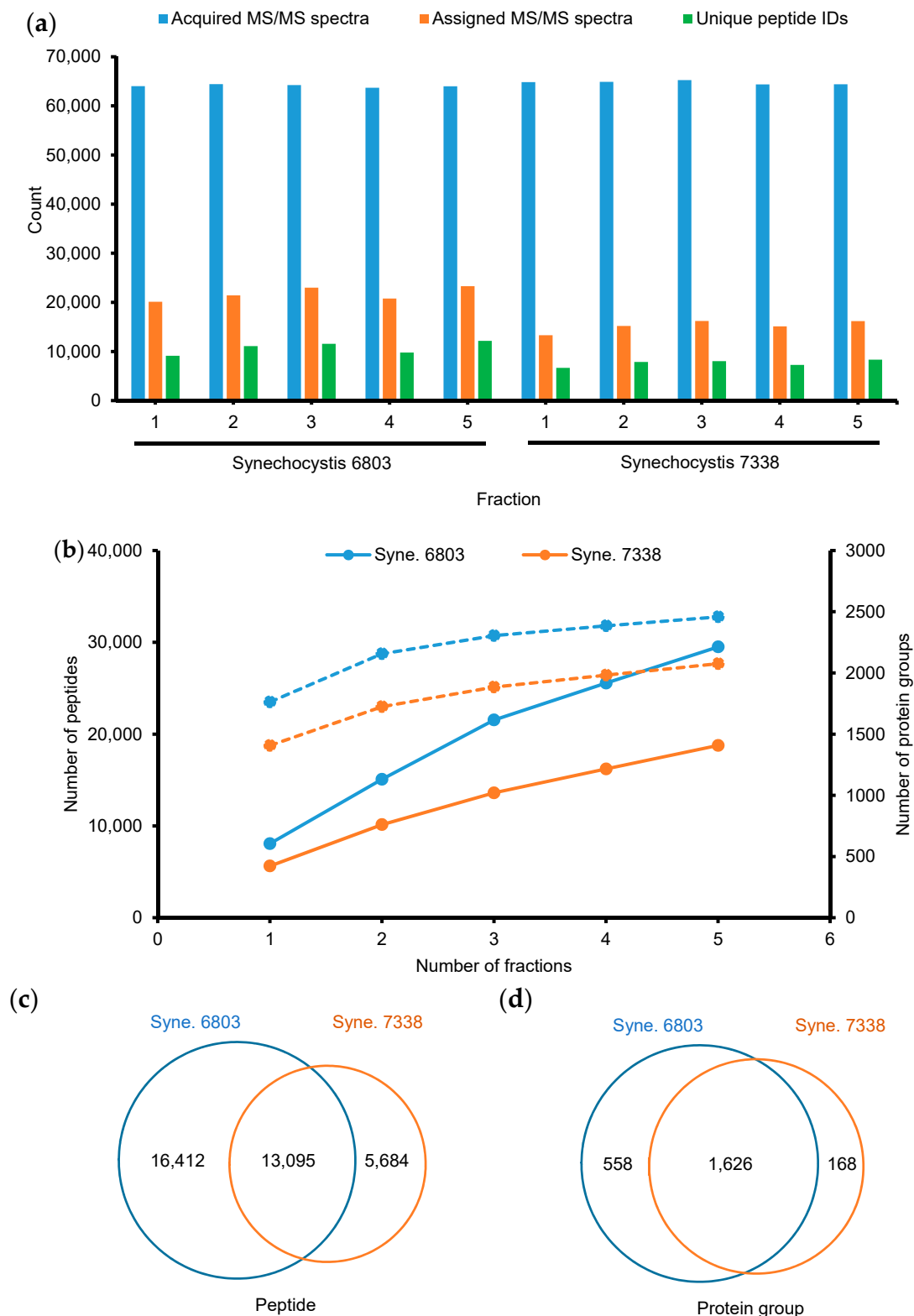


**Figure 1.** Results of the proteomic profiling of *Synechocystis* (Syne.) 6803 and 7338 using the 2D-liquid chromatography (LC) system. (a) Distribution of the number of acquired tandem mass spectrometry (MS/MS) spectra, assigned MS/MS spectra, and unique peptide IDs across five fractions in 2D separation. Samples were proteome digests of *Synechocystis* 6803 and 7338. (b) The cumulative numbers of identified peptides (solid line) and protein groups (single hit included) (dash line) by the number of fractions. (c,d) Venn diagrams that present the numbers of peptides identified with PeptideProphet and protein groups identified with ProteinProphet.

In total, 29,507 and 18,779 unique peptides were identified in *Synechocystis* 6803 and 7338, respectively, whereas the numbers of identified protein groups were 2184 and 1794 (Figure 1c,d). *Synechocystis* 7338 showed slightly fewer identified protein groups due to the use of the *Synechocystis* 6803 database, whereas there may be significant genetic differences between the two strains. The database used for analysis contains a total of 3507 protein groups. Thus, the number of protein groups identified covered 62.3% for *Synechocystis* 6803 and 51.1% for *Synechocystis* 7338. Compared to recent studies, the numbers of identified protein groups were similar [47,48]. As shown in Figure 1d, a total of 168 proteins were not identified in *Synechocystis* 6803 but only identified in *Synechocystis* 7338 as unique proteins for this strain (Table S3). Some of them were factually identified in *Synechocystis* 6803 with one unique peptide and thereby cut off.

The physicochemical properties of the identified peptides in two *Synechocystis* strains were also evaluated. The molecular weight (MW), isoelectric point (pI), and retention time (Rt) of peptides were obtained from TPP. The pI value of a peptide is the value of pH at which the peptide has a net charge of 0. At a pH above pI, the peptide carries a negative charge, and vice versa. The grand average of hydrophathy (GRAVY) values of the peptides were calculated using the GRAVY calculator (<http://gravy-calculator.de/>) [71]. Positive GRAVY values demonstrate hydrophobicity, and negative values indicate hydrophilicity. Figure S1a–d presents the distribution of the MW, pI, GRAVY, and Rt of identified peptides, respectively. Overall, the identified peptides in two *Synechocystis* strains show similar distribution patterns regarding MW, pI, GRAVY, and Rt. For both strains, the majority of the identified peptides have MW values in the range of 800–2200 Da (78–82%), a pI of <7.0 (77–80%), and a GRAVY value of <0.5 (92–93%). The effectiveness of tryptic digestion is shown in Figure S1e. Above 80% of the identified peptides in two strains had two tryptic termini. About 10–12% of the peptides contained 1–2 missed cleavages. Figure S1f exhibits the distribution of proteins by the number of unique peptides. Interestingly, *Synechocystis* 7338 had more proteins with 1–2 unique peptides than *Synechocystis* 6803, which may have resulted from using the *Synechocystis* 6803 database. Figure S1g presents the distribution of proteins by their length, with similar patterns between two strains. About 88% of the proteins were identified with <600 amino acids. The distribution of proteins by coverage (Figure S1h) shows different patterns between *Synechocystis* 6803 and 7338. *Synechocystis* 7338 had more proteins with low coverage (<30%) than *Synechocystis* 6803, which was probably due to an issue with the database.

### 3.2. Comparative Analysis of Quantification Data

DDA selectively chooses and fractionates ions with high intensities, whereas in the DIA method, all of the peptide ions are fragmented. The accuracy, dynamic range, and sensitivity of DIA are similar to those of DDA. However, compared to DDA, DIA can increase the detection of low-abundance proteins [72]. Thus, DIA was utilized to quantify proteins and compare the protein abundance between two *Synechocystis* strains. Four biological replications were used per strain, and *Synechocystis* 7338 was compared against *Synechocystis* 6803. Using Skyline and MSstats, a total of 2049 proteins were quantified and compared (Figure S2). Among them, 396 proteins were defined as differentially expressed proteins (DEPs) and are listed in Table S4 with an adjusted  $p$ -value of  $\leq 0.05$  and  $|\log_2FC|$  of  $\geq 1$ . As shown in the volcano plot (Figure 2a), 211 DEPs were down-expressed and 185 DEPs were up-expressed.

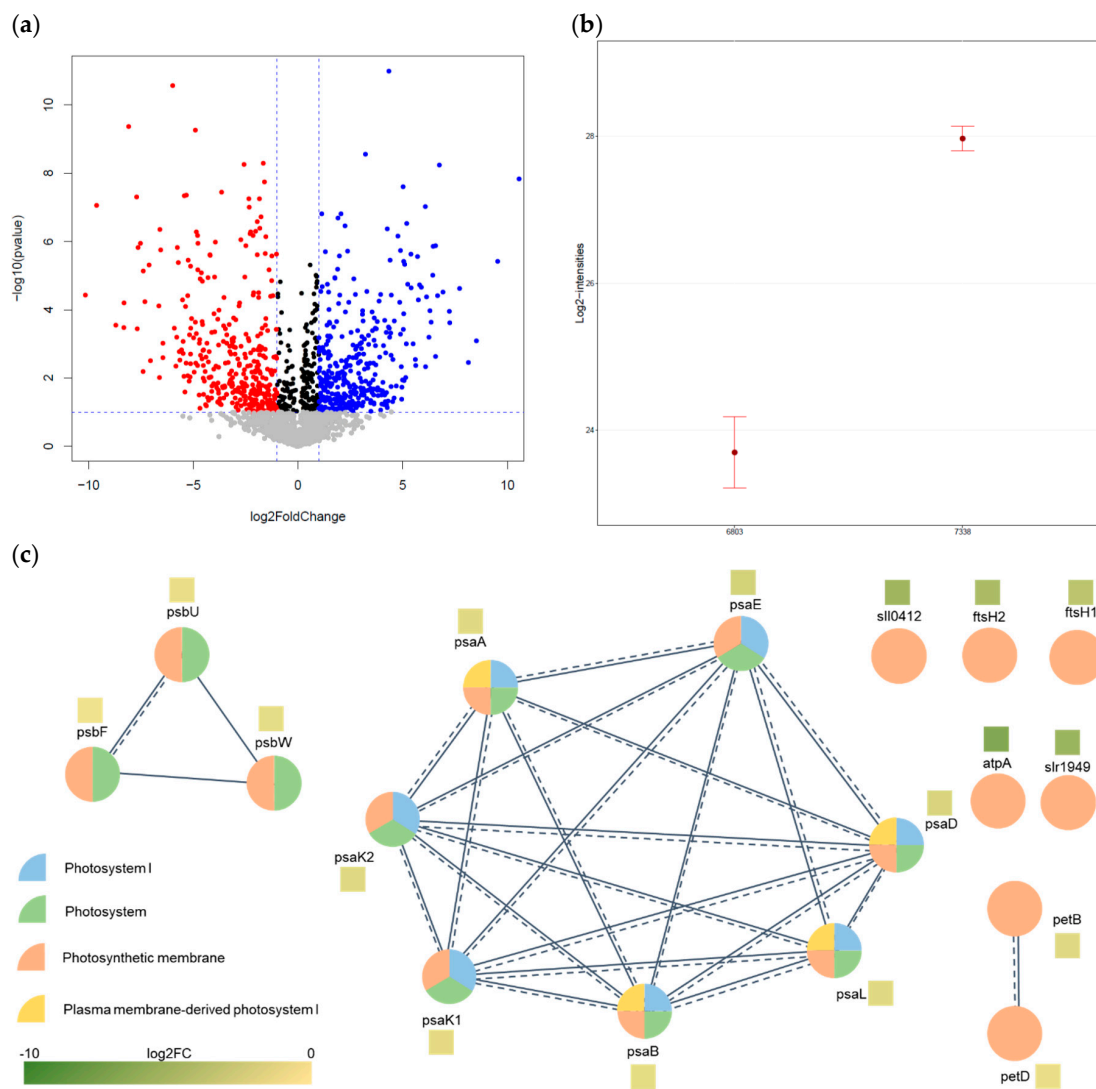


**Figure 2.** (a) Volcano plot illustrating differentially expressed proteins in *Synechocystis* 7338. (b) Comparison of *kdpB* intensities between *Synechocystis* 6803 (left) and 7338 (right). (c) Expression of some down-regulated proteins in *Synechocystis* 7338 relating to photosynthesis and their interactions (via String database). Continuous line: interactions from curated databases; dashed line: interactions from experimental determination.

One of the critical environmental differences between freshwater and sea-based organisms is the osmolality difference depending on the salt concentration. In *Synechocystis*, proteins related to the salt environment adaptation can be assigned into five categories: hypo-osmotic shocks (*aqpZ*, *nhaS*, *kdp*), ion homeostasis (*ktr*, *nhaS*, *kdp*), compatible solute biosynthesis (*ggpS*, *ggpP*, *sps*, *spp*), compatible solute transport (*ggt*), and bioenergetics processes (photosynthesis and respiration) [73]. Some proteins were found in the quantification data (Figure S2), such as *nhaS1* (P73863), *nhaS2* (P74393), *nhaS3* (Q55190), *nhaS5* (Q55736), *kdpB* (P73867), *ggpS* (P74258), *sps* (Q55440), and *ggt* (P74181). Among them, *kdpB*, corresponding to the potassium-transporting ATPase ATP-binding subunit, was significantly up-regulated in *Synechocystis* 7338 (Figure 2b) with a  $\log_2\text{FC}$  value of 4.27. The high-affinity ATP-driven potassium transport system containing this protein is known to facilitate the delivery of potassium into the cytoplasm [74]. In other words, it can be seen as an adaptation of *Synechocystis* 7338 to high-salt-osmotic conductivity under large ion influx. This is probably one of the potential indicators that can be used to distinguish between freshwater and marine *Synechocystis* species.



A number of down-regulated proteins in *Synechocystis* 7338 correspond to the photosynthesis function. In detail, they include 4/6 proteins of plasma membrane-derived photosystem I (psaA-P29254, psaB-P29255, psaD-P19569, and psaL-P37277), 7/14 proteins of photosystem I (psaA, B, D, L, psaE-P12975, psaK1-P72712, and psaK2-P74564), 10/39 proteins of photosystem (seven proteins of photosystem I, psbF-P09191, psbU-Q55332, and psbW-Q55356), and 17/113 proteins of photosynthetic membrane (10 proteins of the photosystem, petB-Q57038, petD-P27589, atpA-P27179, ftsH1-P73179, ftsH2-Q55700, slr1949-P74511, and sll0412-Q55115). The down-regulation of these proteins suggests a reduced photosynthesis function in *Synechocystis* 7338 as compared to that in *Synechocystis* 6803. Figure 2c shows the expression of some down-regulated proteins in *Synechocystis* 7338 relating to photosynthesis and their interactions (from the curated database and experimental determination).

### 3.3. Bioinformatics Analysis

Bioinformatics analysis was conducted using GO and KEGG. The GO database provided by the GO consortium presents a comprehensive computer model of biological systems ranging from molecular levels to larger pathways (cell- and organism-level systems). One of its main functions is the enrichment analysis of units of the gene set. GO analyses of up- and down-regulated proteins are exhibited in Table 1. In addition, the GO analysis of all DEPs was also performed and is presented in Table S5. The down-regulated proteins in *Synechocystis* 7338 relate to various binding functions and several metabolic processes. However, the up-regulated proteins do not reveal any particular GO terms. This is probably due to the use of the *Synechocystis* 6803 database, which does not enable the identification of characteristic proteins in *Synechocystis* 7338. Photosystem I is one of the cellular components corresponding to down-regulated proteins, indicating the reduction of photosynthesis activity in *Synechocystis* 7338. Six proteins in plasma membrane-derived photosystem I are listed in Table 2 with their description,  $\log_2FC$ , and adjusted  $p$ -value. Except for photosystem I reaction center subunit III ( $\log_2FC = -0.263$ ), four proteins (photosystem I reaction center subunit II, XI, photosystem I P700 chlorophyll a apoprotein A1, and A2) were down-regulated, whereas the iron stress-induced chlorophyll-binding protein was up-regulated in *Synechocystis* 7338. Marine cyanobacteria, as aerobic organisms, have several mechanisms for their adaptation to an iron-constrained environment, among which the ATP-binding cassette (ABC) transport system has been known to mediate iron absorption and reduce the function of iron-rich photosystem I [75]. This finding is in agreement with previous studies. During salt stress, the efficiency of photochemistry in *Synechocystis* 6803 decreased due to the down-regulation of almost all genes in the main subunits of photosystem I and II [76,77].

A KEGG analysis was also conducted using the DEPs to reveal metabolic pathways relating to them (Table S6). Table 2 lists the DEPs related to photosynthesis, ABC transporter, and one carbon by folate. The locus names and gene names are expressed as those of *Synechocystis* 6803. NrtB, NrtC, and urea transport system permease proteins (urtC) related to the membrane permeation of nitrogen in *Synechocystis* 7338 were down-regulated, whereas the iron (III) transport system substrate-binding protein was up-regulated. In addition, four down-regulated proteins and two up-regulated proteins were involved in one carbon pool by folate for nitrogen assimilation. Firstly, protein expression related to photosynthesis and amino acid synthesis in *Synechocystis* 6803 was higher than that in *Synechocystis* 7338. This suggests that *Synechocystis* 6803 grows faster than *Synechocystis* 7338 under similar culture conditions because of the increases in protein expression involved in carbon metabolism, photosynthesis, and amino acid synthesis. Differences in protein expression between freshwater and seawater species were also seen in transport metabolism. *Synechocystis* 6803 is known to have a high affinity for N and P in the case of severe nutrient limitations [78]. Nitrate is a nitrogen source for photosynthetic microalgae. It is used for nitrate assimilation by sequentially acting with nitrate reductase and nitrite reductase after uptake by nitrate transport [79]. NrtB encodes a hydrophobic protein with a structural similarity to essential membrane components of ABC transporters. NrtC is known to encode proteins similar to ATP-binding proteins of ABC transporters [80]. Marine cyanobacteria, unlike freshwater species, have been reported to use nrtP or nap permease rather than nrtABCD operon [81]. Transport protein

expression to a nitrogen source showed high urtC expression in the urea uptake system as well as in nitrate transport. Urea is also an important nitrogen source for microalgae. *Synechocystis* 6803 has been reported to be able to take up even small concentrations of urea [82]. Marine cyanobacteria have also been reported to use urea as a nitrogen source [83,84]. However, urtC protein expression of *Synechocystis* 7338 was significantly lower in this study.

**Table 1.** Gene ontology (GO) analysis of differentially expressed proteins in *Synechocystis* 7338.

GO Term	Description	p-Value
<b>Down-Regulated Proteins</b>		
<b>Biological Process</b>		
GO:0008152	Metabolic process	$1.31 \times 10^{-6}$
GO:0071704	Organic substance metabolic process	$2.29 \times 10^{-3}$
GO:0009987	Cellular process	$1.26 \times 10^{-3}$
GO:0044237	Cellular metabolic process	$1.21 \times 10^{-2}$
<b>Cellular Component</b>		
GO:0030094	Plasma membrane-derived photosystem I	$3.54 \times 10^{-2}$
GO:0005737	Cytoplasm	$4.83 \times 10^{-2}$
GO:0044424	Intracellular part	$1.93 \times 10^{-2}$
<b>Molecular Function</b>		
GO:0016462	Pyrophosphatase activity	$4.54 \times 10^{-2}$
GO:0046872	Metal ion binding	$3.15 \times 10^{-2}$
GO:0043168	Anion binding	$6.92 \times 10^{-3}$
GO:0000166	Nucleotide binding	$2.00 \times 10^{-2}$
GO:0036094	Small molecule binding	$1.41 \times 10^{-2}$
GO:0003824	Catalytic activity	$1.28 \times 10^{-7}$
<b>Up-Regulated Proteins</b>		
<b>Biological Process</b>		
GO:0044238	Primary metabolic process	$4.06 \times 10^{-2}$
<b>Cellular Component</b>		
GO:0005737	Cytoplasm	$4.58 \times 10^{-2}$
GO:0005623	Cell	$2.52 \times 10^{-2}$

**Table 2.** Comparison of differentially expressed proteins (DEPs) between *Synechocystis* 6803 and 7338 using GO and Kyoto Encyclopedia of Genes and Genomes (KEGG) analysis.

KEGG Pathway	Locus Name	Gene Name	Protein Description	log <sub>2</sub> FC	Adjusted p-Value
Photosynthesis	<i>slr1834</i>	<i>psaA</i>	Photosystem I P700 chlorophyll a apoprotein A1	-1.761	$1.90 \times 10^{-7}$
	<i>slr1835</i>	<i>psaB</i>	Photosystem I P700 chlorophyll a apoprotein A2	-1.592	$1.79 \times 10^{-8}$
	<i>slr0737</i>	<i>psaD</i>	Photosystem I reaction center subunit II	-2.287	$6.07 \times 10^{-7}$
	<i>sll0819</i>	<i>psaF</i>	Photosystem I reaction center subunit III	-0.263	$4.43 \times 10^{-3}$
	<i>slr1655</i>	<i>psaL</i>	Photosystem I reaction center subunit XI	-1.816	$4.14 \times 10^{-7}$
	<i>sll0247</i>	<i>isiA</i>	Iron stress-induced chlorophyll-binding protein	7.719	$2.43 \times 10^{-5}$
ATP-binding cassette (ABC) transporters	<i>sll1451</i>	<i>nrtB</i>	Nitrate transport protein	-1.527	$2.41 \times 10^{-3}$
	<i>sll1452</i>	<i>nrtC</i>	Nitrate transport protein	-2.396	$2.44 \times 10^{-2}$
	<i>slr0513</i>	<i>sfuA</i>	Iron (III) transport system substrate-binding protein	5.747	$8.82 \times 10^{-4}$
	<i>slr1295</i>			3.228	$1.17 \times 10^{-6}$
	<i>slr1201</i>	<i>urtC</i>	Urea transport system permease protein	-3.068	$2.38 \times 10^{-3}$
One carbon pool by folate	<i>sll0753</i>	<i>folD</i>	Bifunctional NADP-dependent methylene tetrahydrofolate cyclohydrolase/dehydrogenase	-1.271	$3.12 \times 10^{-2}$
	<i>slr0212</i>	<i>metH</i>	Methionine synthase	-2.040	$3.24 \times 10^{-2}$
	<i>sll1635</i>	<i>thyX</i>	Thymidylate synthase	3.642	$2.41 \times 10^{-3}$
	<i>sll0171</i>	<i>gcoT</i>	Aminomethyltransferase	9.540	$1.25 \times 10^{-4}$
	<i>slr0861</i>	<i>purT</i>	Hosphoribosylamine-glycine ligase	-7.698	$6.82 \times 10^{-6}$
	<i>slr0477</i>	<i>purN</i>		-4.239	$1.23 \times 10^{-2}$

C1 metabolism showed the protein expression using different pathways in one metabolism process. C1 metabolism plays a major role in the supply and reproduction of methyl groups. It is essential to produce amino acids such as methionine, glycine, and serine, as well as purine and thymidylate [85]. As shown in Figure 3, *Synechocystis* 6803 converted 5,10-methylene-tetrahydrofolate (5,10-methylene-THF) to 5,10-methenyl-THF through methenyltetrahydrofolate cyclohydrolase, and 5,10-methenyl-THF was converted to 10-formyl-THF by methylenetetrahydrofolate dehydrogenase, while 10-formyl-THF was converted to formate by reproducing THF. In comparison, aminomethyltransferase (GDC) and thymidylate synthase in *Synechocystis* 7338 are known to convert 5,10-methylene-THF into glycine. GDC in *Synechocystis* 6803 has been reported as a non-essential gene since the GDC-deleted mutant did not hinder its growth using C1 metabolism without GDC [86]. GDC is located in the mitochondria of eukaryotic cells and is known to be involved in photorespiration and nitrate assimilation [85,87]. In plants, GDC also acts as a feedback signal that regulates carbon flow in photosynthesis and photorespiration while being regulated by glycine levels [88,89]. Moreover, GDC deficient plants are known to cause an over-reduction and over-energizing of chloroplasts due to their dysregulation of photorespiration [90]. In marine organisms, glycine is known to be an amino acid-based osmolyte that is produced to control intracellular osmotic pressure [91]. Therefore, *Synechocystis* 7338 seems to use osmolyte glycine as a substrate for C1 metabolism to regulate carbon flow, unlike *Synechocystis* 6803.

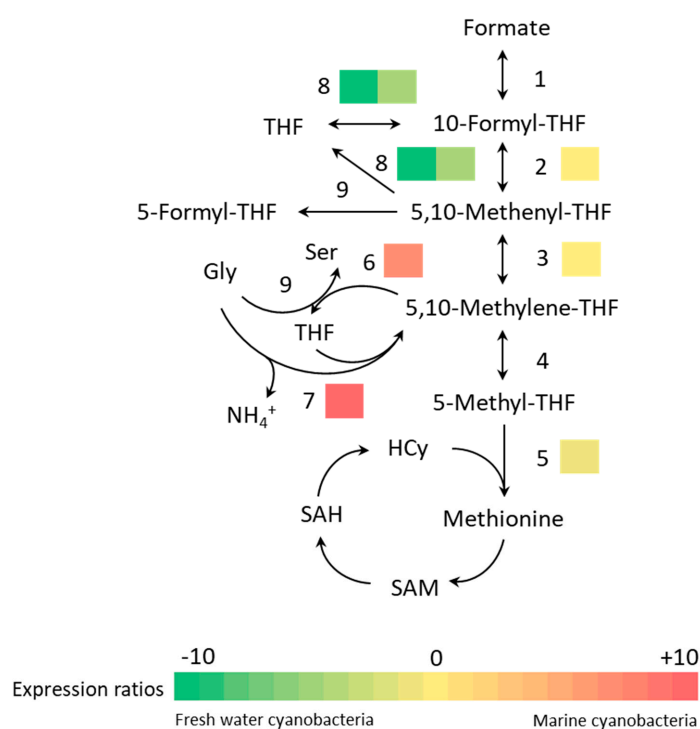


**Figure 3.** Comparison of protein expressions in one-carbon metabolism between *Synechocystis* 6803 and 7338. The enzymes are (1) 10-formyl-THF synthetase, (2,3) bifunctional NADP-dependent methylene-THF cyclohydrolase/dehydrogenase, (4) NADH-dependent methylene-THF reductase, (5) methionine synthase, (6) serine hydroxymethyltransferase, (7) aminomethyltransferase (GDC), (8) phosphoribosylamine-glycine ligase, and (9) serine hydroxymethyl transferase. Abbreviations: THF, tetrahydrofolate; Hcy, homocysteine; SAH, S-adenosyl-homocysteine; SAM, S-adenosyl-methionine.

#### 4. Conclusions

In this study, proteomic profiling of *Synechocystis* 7338 was performed for the first time. Through qualitative and quantitative analyses, proteomes of *Synechocystis* 6803 and 7338 were compared. Our findings revealed some characteristics of the proteome, such as its adaptation to living

conditions. *Synechocystis* 7338 differed from the freshwater strain by the reduced expression of some photosynthesis proteins as well as the up-regulation of kdpB. In C1 metabolism, *Synechocystis* 7338 may use osmolyte glycine as a substrate to regulate carbon flow. Further studies should be conducted on *Synechocystis* 7338, particularly regarding its genomics and transcriptomics. As its genome is available, the proteomic data in this study can be re-analyzed to obtain an insight into its proteomic profile and reveal the in-depth proteomic differences of this marine strain in comparison with the freshwater strain.

**Supplementary Materials:** The following are available online at <http://www.mdpi.com/2077-1312/8/10/790/s1>, Figure S1: Comparison of features of peptides and proteins identified in DDA MS between *Synechocystis* 6803 and 7338, Figure S2: Protein intensities quantified using Skyline, Table S1: List of identified peptides (PeptideProphet) in *Synechocystis* 6803 and 7338 using DDA MS, Table S2: List of identified proteins (ProteinProphet) in *Synechocystis* 6803 and 7338, Table S3: List of unique and shared proteins (ProteinProphet) of *Synechocystis* 6803 and 7338, Table S4: Differentially expressed proteins in *Synechocystis* 7338 compared with *Synechocystis* 6803, Table S5: Gene ontology analysis of differentially expressed proteins in *Synechocystis* 7338, Table S6: KEGG pathways relating to differentially expressed proteins in *Synechocystis* 7338. The proteomics data have been deposited to the ProteomeXchange Consortium via the PRIDE partner repository with the dataset identifier PXD019340. Reviewers may access it using username reviewer96059@ebi.ac.uk and password jNWAatQQM.

**Author Contributions:** Conceptualization, B.-K.C., C.-G.L., H.-K.C. and H.L.; methodology, J.-M.P. and H.L.; validation, J.-M.P. and V.-A.D.; formal analysis, D.K. and V.-A.D.; investigation, D.K., S.-J.H., and D.-M.K.; resources, J.-M.P. and B.-K.C.; data curation, D.K. and V.-A.D.; writing—original draft preparation, D.K., S.-J.H., B.-K.C., C.-G.L., and H.-K.C.; writing—review and editing, V.-A.D. and H.L.; visualization, D.K., V.-A.D., and S.-J.H.; supervision, J.-M.P.; project administration, H.L.; funding acquisition, H.L. All authors have read and agreed to the published version of the manuscript.

**Funding:** This work was supported by the National Research Foundation of Korea (NRF) grant, funded by the Korea government (MSIT) (NRF-2017M3D9A1073784) and the Health Fellowship Foundation.

**Conflicts of Interest:** The authors declare no conflict of interest. The funders had no role in the design of the study; in the collection, analyses, or interpretation of data; in the writing of the manuscript, or in the decision to publish the results.

## References

- Georgianna, D.R.; Mayfield, S.P. Exploiting diversity and synthetic biology for the production of algal biofuels. *Nature* **2012**, *488*, 329–335. [[CrossRef](#)]
- Hondo, S.; Takahashi, M.; Osanai, T.; Matsuda, M.; Hasunuma, T.; Tazuke, A.; Nakahira, Y.; Chohnan, S.; Hasegawa, M.; Asayama, M. Genetic engineering and metabolite profiling for overproduction of polyhydroxybutyrate in cyanobacteria. *J. Biosci. Bioeng.* **2015**, *120*, 510–517. [[CrossRef](#)]
- Bonnard, I.; Bornancin, L.; Dalle, K.; Chinain, M.; Zubia, M.; Banaigs, B.; Roué, M. Assessment of the Chemical diversity and potential toxicity of benthic cyanobacterial blooms in the Lagoon of Moorea Island (French Polynesia). *J. Mar. Sci. Eng.* **2020**, *8*, 406. [[CrossRef](#)]
- De Santi, F.; Luciani, G.; Bresciani, M.; Giardino, C.; Lovergine, F.P.; Pasquariello, G.; Vaiciute, D.; De Carolis, G. Synergistic Use of synthetic aperture radar and optical imagery to monitor surface accumulation of cyanobacteria in the Curonian Lagoon. *J. Mar. Sci. Eng.* **2019**, *7*, 461. [[CrossRef](#)]
- Pagliara, P.; Barca, A.; Verri, T.; Caroppo, C. The Marine Sponge *Petrosia ficiformis* Harbors Different Cyanobacteria Strains with Potential Biotechnological Application. *J. Mar. Sci. Eng.* **2020**, *8*, 638. [[CrossRef](#)]
- Wahlen, B.D.; Willis, R.M.; Seefeldt, L.C. Biodiesel production by simultaneous extraction and conversion of total lipids from microalgae, cyanobacteria, and wild mixed-cultures. *Bioresour. Technol.* **2011**, *102*, 2724–2730. [[CrossRef](#)] [[PubMed](#)]
- Janasch, M.; Asplund-Samuelsson, J.; Steuer, R.; Hudson, E.P. Kinetic modeling of the Calvin cycle identifies flux control and stable metabolomes in *Synechocystis* carbon fixation. *J. Exp. Bot.* **2018**, *70*, 973–983. [[CrossRef](#)]
- Kłodawska, K.; Kovács, L.; Vladkova, R.; Rzaska, A.; Gombos, Z.; Laczko-Dobos, H.; Malec, P. Trimeric organization of photosystem I is required to maintain the balanced photosynthetic electron flow in cyanobacterium *Synechocystis* sp. PCC 6803. *Photosynth. Res.* **2020**, *143*, 251–262. [[CrossRef](#)]
- Cheregi, O.; Funk, C. Regulation of the scp Genes in the Cyanobacterium *Synechocystis* sp. PCC 6803—What is New? *Molecules* **2015**, *20*, 14621–14637. [[CrossRef](#)] [[PubMed](#)]
- Angermayr, S.A.; Hellingwerf, K.J.; Lindblad, P.; Teixeira De Mattos, M.J. Energy biotechnology with cyanobacteria. *Curr. Opin. Biotechnol.* **2009**, *20*, 257–263. [[CrossRef](#)]

11. Hannon, M.; Gimpel, J.; Tran, M.; Rasala, B.; Mayfield, S. Biofuels from algae: Challenges and potential. *Biofuels* **2010**, *1*, 763–784. [[CrossRef](#)] [[PubMed](#)]
12. Nozzi, N.E.; Oliver, J.W.K.; Atsumi, S. Cyanobacteria as a Platform for Biofuel Production. *Front. Bioeng. Biotechnol.* **2013**, *1*. [[CrossRef](#)]
13. Sarsekeyeva, F.; Zayadan, B.K.; Usserbaeva, A.; Bedbenov, V.S.; Sinetova, M.A.; Los, D.A. Cyanofuels: Biofuels from cyanobacteria. Reality and perspectives. *Photosynth. Res.* **2015**, *125*, 329–340. [[CrossRef](#)]
14. Ikeuchi, M.; Tabata, S. *Synechocystis* sp. PCC 6803—A useful tool in the study of the genetics of cyanobacteria. *Photosynth. Res.* **2001**, *70*, 73–83. [[CrossRef](#)]
15. Wijffels, R.H.; Kruse, O.; Hellingwerf, K.J. Potential of industrial biotechnology with cyanobacteria and eukaryotic microalgae. *Curr. Opin. Biotechnol.* **2013**, *24*, 405–413. [[CrossRef](#)] [[PubMed](#)]
16. Giner-Lamia, J.; López-Maury, L.; Florencio, F.J. Global Transcriptional Profiles of the Copper Responses in the Cyanobacterium *Synechocystis* sp. PCC 6803. *PLoS ONE* **2014**, *9*, e108912. [[CrossRef](#)] [[PubMed](#)]
17. Giner-Lamia, J.; López-Maury, L.; Reyes, J.C.; Florencio, F.J. The CopRS Two-Component System Is Responsible for Resistance to Copper in the Cyanobacterium *Synechocystis* sp. PCC 6803. *Plant Physiol.* **2012**, *159*, 1806–1818. [[CrossRef](#)] [[PubMed](#)]
18. Nagarajan, S.; Srivastava, S.; Sherman, L.A. Essential role of the plasmid hik31 operon in regulating central metabolism in the dark in *Synechocystis* sp. PCC 6803. *Mol. Microbiol.* **2014**, *91*, 79–97. [[CrossRef](#)]
19. Ikeuchi, M. Complete genome sequence of a cyanobacterium *Synechocystis* sp. PCC 6803, the oxygenic photosynthetic prokaryote. *Protein Nucleic Acid Enzyme* **1996**, *41*, 2579–2583.
20. Chen, Z.; Li, X.; Tan, X.; Zhang, Y.; Wang, B. Recent Advances in Biological functions of thick pili in the cyanobacterium *Synechocystis* sp. PCC 6803. *Front. Plant Sci.* **2020**, *11*. [[CrossRef](#)]
21. Liu, X.; Sheng, J.; Curtiss, R., III. Fatty acid production in genetically modified cyanobacteria. *Proc. Natl. Acad. Sci. USA* **2011**, *108*, 6899–6904. [[CrossRef](#)] [[PubMed](#)]
22. Tan, X.; Yao, L.; Gao, Q.; Wang, W.; Qi, F.; Lu, X. Photosynthesis driven conversion of carbon dioxide to fatty alcohols and hydrocarbons in cyanobacteria. *Metab. Eng.* **2011**, *13*, 169–176. [[CrossRef](#)] [[PubMed](#)]
23. Dexter, J.; Fu, P. Metabolic engineering of cyanobacteria for ethanol production. *Energy Environ. Sci.* **2009**, *2*, 857–864. [[CrossRef](#)]
24. Lee, B.D.; Apel, W.A.; Walton, M.R. Screening of Cyanobacterial Species for Calcification. *Biotechnol. Prog.* **2004**, *20*, 1345–1351. [[CrossRef](#)] [[PubMed](#)]
25. Tan, L.T. Bioactive natural products from marine cyanobacteria for drug discovery. *Phytochemistry* **2007**, *68*, 954–979. [[CrossRef](#)] [[PubMed](#)]
26. Nunnery, J.K.; Mevers, E.; Gerwick, W.H. Biologically active secondary metabolites from marine cyanobacteria. *Curr. Opin. Biotechnol.* **2010**, *21*, 787–793. [[CrossRef](#)] [[PubMed](#)]
27. Noh, Y.; Lee, H.; Hong, S.-J.; Lee, H.; Cho, B.-K.; Lee, C.-G.; Choi, H.-K. Comparative primary metabolic and lipidomic profiling of freshwater and marine *Synechocystis* strains using by GC-MS and NanoESI-MS analyses. *Biotechnol. Bioprocess Eng.* **2020**, *25*, 308–319. [[CrossRef](#)]
28. Herreros-Cabello, A.; Callejas-Hernández, F.; Fresno, M.; Gironès, N. Comparative proteomic analysis of trypanomastigotes from *Trypanosoma cruzi* strains with different pathogenicity. *Infect. Genet. Evol.* **2019**, *76*, 104041. [[CrossRef](#)]
29. Elhosseiny, N.M.; Elhezawy, N.B.; Attia, A.S. Comparative proteomics analyses of *Acinetobacter baumannii* strains ATCC 17978 and AB5075 reveal the differential role of type II secretion system secretomes in lung colonization and ciprofloxacin resistance. *Microb. Pathog.* **2019**, *128*, 20–27. [[CrossRef](#)]
30. Battchikova, N.; Muth-Pawlak, D.; Aro, E.-M. Proteomics of cyanobacteria: Current horizons. *Curr. Opin. Biotechnol.* **2018**, *54*, 65–71. [[CrossRef](#)]
31. Gao, L.; Wang, J.; Ge, H.; Fang, L.; Zhang, Y.; Huang, X.; Wang, Y. Toward the complete proteome of *Synechocystis* sp. PCC 6803. *Photosynth. Res.* **2015**, *126*, 203–219. [[CrossRef](#)] [[PubMed](#)]
32. Huang, F.; Hedman, E.; Funk, C.; Kieselbach, T.; Schröder, W.P.; Norling, B. Isolation of Outer Membrane of *Synechocystis* sp. PCC 6803 and Its Proteomic Characterization. *Mol. Cell. Proteom.* **2004**, *3*, 586–595. [[CrossRef](#)] [[PubMed](#)]
33. Slabas, A.R.; Suzuki, I.; Murata, N.; Simon, W.J.; Hall, J.J. Proteomic analysis of the heat shock response in *Synechocystis* PCC6803 and a thermally tolerant knockout strain lacking the histidine kinase 34 gene. *Proteomics* **2006**, *6*, 845–864. [[CrossRef](#)] [[PubMed](#)]



34. Gao, Y.; Xiong, W.; Li, X.-B.; Gao, C.-F.; Zhang, Y.-L.; Li, H.; Wu, Q.-Y. Identification of the proteomic changes in *Synechocystis* sp. PCC 6803 following prolonged UV-B irradiation. *J. Exp. Bot.* **2009**, *60*, 1141–1154. [[CrossRef](#)] [[PubMed](#)]
35. Rowland, J.G.; Simon, W.J.; Prakash, J.S.S.; Slabas, A.R. Proteomics reveals a role for the RNA helicase crhR in the modulation of multiple metabolic pathways during cold acclimation of *synechocystis* sp. PCC6803. *J. Proteome Res.* **2011**, *10*, 3674–3689. [[CrossRef](#)] [[PubMed](#)]
36. Fulda, S.; Mikkat, S.; Huang, F.; Huckauf, J.; Marin, K.; Norling, B.; Hagemann, M. Proteome analysis of salt stress response in the cyanobacterium *Synechocystis* sp. strain PCC 6803. *Proteomics* **2006**, *6*, 2733–2745. [[CrossRef](#)] [[PubMed](#)]
37. Wegener, K.M.; Singh, A.K.; Jacobs, J.M.; Elvitigala, T.; Welsh, E.A.; Keren, N.; Gritsenko, M.A.; Ghosh, B.K.; Camp, D.G.; Smith, R.D.; et al. Global Proteomics Reveal an Atypical Strategy for Carbon/Nitrogen Assimilation by a Cyanobacterium Under Diverse Environmental Perturbations. *Mol. Cell. Proteom.* **2010**, *9*, 2678–2689. [[CrossRef](#)] [[PubMed](#)]
38. Angeleri, M.; Muth-Pawlak, D.; Wilde, A.; Aro, E.-M.; Battchikova, N. Global proteome response of *Synechocystis* 6803 to extreme copper environments applied to control the activity of the inducible petJ promoter. *J. Appl. Microbiol.* **2019**, *126*, 826–841. [[CrossRef](#)]
39. Spät, P.; Klotz, A.; Rexroth, S.; Maček, B.; Forchhammer, K. Chlorosis as a Developmental Program in Cyanobacteria: The Proteomic Fundament for Survival and Awakening. *Mol. Cell. Proteom.* **2018**, *17*, 1650–1669. [[CrossRef](#)]
40. Baers, L.L.; Breckels, L.M.; Mills, L.A.; Gatto, L.; Deery, M.J.; Stevens, T.J.; Howe, C.J.; Lilley, K.S.; Lea-Smith, D.J. Proteome Mapping of a Cyanobacterium Reveals Distinct Compartment Organization and Cell-Dispersed Metabolism. *Plant Physiol.* **2019**, *181*, 1721–1738. [[CrossRef](#)]
41. Cui, M.; Liu, Y.; Zhang, J. Sulfamethoxazole and tetracycline induced alterations in biomass, photosynthesis, lipid productivity, and proteomic expression of *Synechocystis* sp. PCC 6803. *Environ. Sci. Pollut. Res.* **2020**, *27*, 30437–30447. [[CrossRef](#)] [[PubMed](#)]
42. Talamantes, T.; Ughy, B.; Domonkos, I.; Kis, M.; Gombos, Z.; Prokai, L. Label-free LC-MS/MS identification of phosphatidylglycerol-regulated proteins in *Synechocystis* sp. PCC6803. *Proteomics* **2014**, *14*, 1053–1057. [[CrossRef](#)] [[PubMed](#)]
43. Gao, L.; Ge, H.; Huang, X.; Liu, K.; Zhang, Y.; Xu, W.; Wang, Y. Systematically Ranking the Tightness of Membrane Association for Peripheral Membrane Proteins (PMPs). *Mol. Cell. Proteom.* **2015**, *14*, 340–353. [[CrossRef](#)] [[PubMed](#)]
44. Qiao, J.; Wang, J.; Chen, L.; Tian, X.; Huang, S.; Ren, X.; Zhang, W. Quantitative iTRAQ LC–MS/MS Proteomics reveals metabolic responses to biofuel ethanol in cyanobacterial *synechocystis* sp. PCC 6803. *J. Proteome Res.* **2012**, *11*, 5286–5300. [[CrossRef](#)]
45. Liu, J.; Chen, L.; Wang, J.; Qiao, J.; Zhang, W. Proteomic analysis reveals resistance mechanism against biofuel hexane in *Synechocystis* sp. PCC 6803. *Biotechnol. Biofuels* **2012**, *5*, 68. [[CrossRef](#)]
46. Huang, S.; Chen, L.; Te, R.; Qiao, J.; Wang, J.; Zhang, W. Complementary iTRAQ proteomics and RNA-seq transcriptomics reveal multiple levels of regulation in response to nitrogen starvation in *Synechocystis* sp. PCC 6803. *Mol. Biosyst.* **2013**, *9*, 2565–2574. [[CrossRef](#)]
47. Tian, X.; Chen, L.; Wang, J.; Qiao, J.; Zhang, W. Quantitative proteomics reveals dynamic responses of *Synechocystis* sp. PCC 6803 to next-generation biofuel butanol. *J. Proteom.* **2013**, *78*, 326–345. [[CrossRef](#)]
48. Chen, L.; Wu, L.; Wang, J.; Zhang, W. Butanol tolerance regulated by a two-component response regulator Slr1037 in photosynthetic *Synechocystis* sp. PCC 6803. *Biotechnol. Biofuels* **2014**, *7*, 89. [[CrossRef](#)]
49. Song, Z.; Chen, L.; Wang, J.; Lu, Y.; Jiang, W.; Zhang, W. A Transcriptional Regulator Sll0794 Regulates Tolerance to Biofuel Ethanol in Photosynthetic *Synechocystis* sp. PCC 6803. *Mol. Cell. Proteom.* **2014**, *13*, 3519–3532. [[CrossRef](#)]
50. Krynická, V.; Georg, J.; Jackson, P.J.; Dickman, M.J.; Hunter, C.N.; Futschik, M.E.; Hess, W.R.; Komenda, J. Depletion of the FtsH1/3 Proteolytic complex suppresses the nutrient stress response in the cyanobacterium *synechocystis* sp strain PCC 6803. *Plant Cell* **2019**, *31*, 2912–2928. [[CrossRef](#)]
51. Solymosi, D.; Nikkanen, L.; Muth-Pawlak, D.; Fitzpatrick, D.; Vasudevan, R.; Howe, C.J.; Lea-Smith, D.J.; Allahverdiyeva, Y. Cytochrome cM decreases photosynthesis under photomixotrophy in *synechocystis* sp. PCC 6803. *Plant Physiol.* **2020**, *183*, 700–716. [[CrossRef](#)] [[PubMed](#)]

52. Toyoshima, M.; Tokumaru, Y.; Matsuda, F.; Shimizu, H. Assessment of protein content and phosphorylation level in *synechocystis* sp. PCC 6803 under various growth conditions using quantitative phosphoproteomic analysis. *Molecules* **2020**, *25*, 3582. [[CrossRef](#)] [[PubMed](#)]
53. Svensson, M.; Borén, M.; Sköld, K.; Fälth, M.; Sjögren, B.; Andersson, M.; Svenningsson, P.; Andrén, P.E. Heat stabilization of the tissue proteome: A new technology for improved proteomics. *J. Proteome Res.* **2009**, *8*, 974–981. [[CrossRef](#)] [[PubMed](#)]
54. Van-An, D.; Jeeyun, A.; Na-Young, H.; Jong-Moon, P.; Jeong-Hun, M.; Tae Wan, K.; Hookeun, L. Proteomic Analysis of the vitreous body in proliferative and non-proliferative diabetic retinopathy. *Curr. Proteom.* **2020**, *17*. [[CrossRef](#)]
55. Yun, G.; Park, J.-M.; Duong, V.-A.; Mok, J.-H.; Jeon, J.; Nam, O.; Lee, J.; Jin, E.; Lee, H. Proteomic profiling of *emiliana huxleyi* using a three-dimensional separation method combined with tandem mass spectrometry. *Molecules* **2020**, *25*, 3028. [[CrossRef](#)] [[PubMed](#)]
56. Dwivedi, R.C.; Spicer, V.; Harder, M.; Antonovici, M.; Ens, W.; Standing, K.G.; Wilkins, J.A.; Krokhin, O.V. Practical implementation of 2D HPLC scheme with accurate peptide retention prediction in both dimensions for high-throughput bottom-up proteomics. *Anal. Chem.* **2008**, *80*, 7036–7042. [[CrossRef](#)]
57. Perez-Riverol, Y.; Csordas, A.; Bai, J.; Bernal-Llinares, M.; Hewapathirana, S.; Kundu, D.J.; Inuganti, A.; Griss, J.; Mayer, G.; Eisenacher, M.; et al. The PRIDE database and related tools and resources in 2019: Improving support for quantification data. *Nucleic Acids Res.* **2018**, *47*, D442–D450. [[CrossRef](#)]
58. Eng, J.K.; Jahan, T.A.; Hoopmann, M.R. Comet: An open-source MS/MS sequence database search tool. *Proteomics* **2013**, *13*, 22–24. [[CrossRef](#)]
59. Deutsch, E.W.; Mendoza, L.; Shteynberg, D.; Slagel, J.; Sun, Z.; Moritz, R.L. Trans-Proteomic Pipeline, a standardized data processing pipeline for large-scale reproducible proteomics informatics. *Proteom. Clin. Appl.* **2015**, *9*, 745–754. [[CrossRef](#)]
60. Keller, A.; Nesvizhskii, A.I.; Kolker, E.; Aebersold, R. Empirical Statistical Model To Estimate the Accuracy of Peptide Identifications Made by MS/MS and Database Search. *Anal. Chem.* **2002**, *74*, 5383–5392. [[CrossRef](#)]
61. Nesvizhskii, A.I.; Keller, A.; Kolker, E.; Aebersold, R. A Statistical model for identifying proteins by tandem mass spectrometry. *Anal. Chem.* **2003**, *75*, 4646–4658. [[CrossRef](#)] [[PubMed](#)]
62. Pino, L.K.; Searle, B.C.; Bollinger, J.G.; Nunn, B.; MacLean, B.; MacCoss, M.J. The Skyline ecosystem: Informatics for quantitative mass spectrometry proteomics. *Mass Spectrom. Rev.* **2020**, *39*, 229–244. [[CrossRef](#)] [[PubMed](#)]
63. Jong-Moon, P.; Van-An, D.; Jeong-Hun, M.; Doo-Jin, C.; Hookeun, L. A Quantitative Proteomic Analysis to Reveal Effects of N-acetylcysteine on H<sub>2</sub>O<sub>2</sub>-induced Cytotoxicity. *Curr. Proteom.* **2020**, *17*, 1–13. [[CrossRef](#)]
64. Choi, M.; Chang, C.-Y.; Clough, T.; Broudy, D.; Killeen, T.; MacLean, B.; Vitek, O. MSstats: An R package for statistical analysis of quantitative mass spectrometry-based proteomic experiments. *Bioinformatics* **2014**, *30*, 2524–2526. [[CrossRef](#)] [[PubMed](#)]
65. Ashburner, M.; Ball, C.A.; Blake, J.A.; Botstein, D.; Butler, H.; Cherry, J.M.; Davis, A.P.; Dolinski, K.; Dwight, S.S.; Eppig, J.T.; et al. Gene Ontology: Tool for the unification of biology. *Nat. Genet.* **2000**, *25*, 25–29. [[CrossRef](#)]
66. Kanehisa, M.; Goto, S.; Kawashima, S.; Nakaya, A. The KEGG databases at GenomeNet. *Nucleic Acids Res.* **2002**, *30*, 42–46. [[CrossRef](#)]
67. Szklarczyk, D.; Gable, A.L.; Lyon, D.; Junge, A.; Wyder, S.; Huerta-Cepas, J.; Simonovic, M.; Doncheva, N.T.; Morris, J.H.; Bork, P.; et al. STRING v11: Protein–protein association networks with increased coverage, supporting functional discovery in genome-wide experimental datasets. *Nucleic Acids Res.* **2018**, *47*, D607–D613. [[CrossRef](#)]
68. Tiwary, S.; Levy, R.; Gutenbrunner, P.; Salinas Soto, F.; Palaniappan, K.K.; Deming, L.; Berndl, M.; Brant, A.; Cimermancic, P.; Cox, J. High-quality MS/MS spectrum prediction for data-dependent and data-independent acquisition data analysis. *Nat. Methods* **2019**, *16*, 519–525. [[CrossRef](#)]
69. Duong, V.-A.; Park, J.-M.; Lee, H. Review of three-dimensional liquid chromatography platforms for bottom-up proteomics. *Int. J. Mol. Sci.* **2020**, *21*, 1524. [[CrossRef](#)]
70. Yang, F.; Shen, Y.; Camp, D.G.; Smith, R.D. High-pH reversed-phase chromatography with fraction concatenation for 2D proteomic analysis. *Expert Rev. Proteom.* **2012**, *9*, 129–134. [[CrossRef](#)]

71. Chen, D.; Shen, X.; Sun, L. Strong cation exchange-reversed phase liquid chromatography-capillary zone electrophoresis-tandem mass spectrometry platform with high peak capacity for deep bottom-up proteomics. *Anal. Chim. Acta* **2018**, *1012*, 1–9. [[CrossRef](#)] [[PubMed](#)]
72. Hu, A.; Noble, W.S.; Wolf-Yadlin, A. Technical advances in proteomics: New developments in data-independent acquisition. *F1000Research* **2016**, *5*, 419. [[CrossRef](#)] [[PubMed](#)]
73. Hagemann, M. Molecular biology of cyanobacterial salt acclimation. *FEMS Microbiol. Rev.* **2011**, *35*, 87–123. [[CrossRef](#)] [[PubMed](#)]
74. Nanatani, K.; Shijuku, T.; Takano, Y.; Zulkifli, L.; Yamazaki, T.; Tominaga, A.; Souma, S.; Onai, K.; Morishita, M.; Ishiura, M.; et al. Comparative analysis of kdp and ktr mutants reveals distinct roles of the potassium transporters in the model cyanobacterium *Synechocystis* sp. strain PCC 6803. *J. Bacteriol.* **2015**, *197*, 676–687. [[CrossRef](#)] [[PubMed](#)]
75. Morrissey, J.; Bowler, C. Iron utilization in marine cyanobacteria and eukaryotic algae. *Front. Microbiol.* **2012**, *3*. [[CrossRef](#)] [[PubMed](#)]
76. Marin, K.; Kanesaki, Y.; Los, D.A.; Murata, N.; Suzuki, I.; Hagemann, M. Gene Expression Profiling Reflects Physiological Processes in Salt Acclimation of *Synechocystis* sp. Strain PCC 6803. *Plant Physiol.* **2004**, *136*, 3290–3300. [[CrossRef](#)]
77. Kanesaki, Y.; Suzuki, I.; Allakhverdiev, S.I.; Mikami, K.; Murata, N. Salt Stress and Hyperosmotic Stress Regulate the Expression of Different Sets of Genes in *Synechocystis* sp. PCC 6803. *Biochem. Biophys. Res. Commun.* **2002**, *290*, 339–348. [[CrossRef](#)]
78. Lee, R.E. *Phycology*; Cambridge University Press: New York, NY, USA, 2012; pp. 33–80.
79. Kobayashi, M.; Takatani, N.; Tanigawa, M.; Omata, T. Posttranslational Regulation of Nitrate Assimilation in the Cyanobacterium *Synechocystis* sp. Strain PCC 6803. *J. Bacteriol.* **2005**, *187*, 498–506. [[CrossRef](#)]
80. Maeda, S.I.; Omata, T. Substrate-binding Lipoprotein of the Cyanobacterium *Synechococcus* sp. Strain PCC 7942 Involved in the Transport of Nitrate and Nitrite. *J. Biol. Chem.* **1997**, *272*, 3036–3041. [[CrossRef](#)]
81. Herrero, A.; Muro-Pastor, A.M.; Flores, E. Nitrogen Control in Cyanobacteria. *J. Bacteriol.* **2001**, *183*, 411–425. [[CrossRef](#)]
82. Valladares, A.; Montesinos, M.L.; Herrero, A.; Flores, E. An ABC-type, high-affinity urea permease identified in cyanobacteria. *Mol. Microbiol.* **2002**, *43*, 703–715. [[CrossRef](#)] [[PubMed](#)]
83. Collier, J.L.; Brahmasha, B.; Palenik, B. The marine cyanobacterium *Synechococcus* sp. WH7805 requires urease (urea amidohydrolase, EC 3.5.1.5) to utilize urea as a nitrogen source: Molecular-genetic and biochemical analysis of the enzyme. *Microbiology* **1999**, *145*, 447–459. [[CrossRef](#)] [[PubMed](#)]
84. Moore, L.R.; Post, A.F.; Rocop, G.; Chisholm, S.W. Utilization of different nitrogen sources by the marine cyanobacteria *Prochlorococcus* and *Synechococcus*. *Limnol. Oceanogr.* **2002**, *47*, 989–996. [[CrossRef](#)]
85. Maurino, V.G.; Peterhansel, C. Photorespiration: Current status and approaches for metabolic engineering. *Curr. Opin. Plant Biol.* **2010**, *13*, 248–255. [[CrossRef](#)] [[PubMed](#)]
86. Hagemann, M.; Vinnemeier, J.; Oberpichler, I.; Boldt, R.; Bauwe, H. The Glycine Decarboxylase Complex is not Essential for the Cyanobacterium *Synechocystis* sp. Strain PCC 6803. *Plant Biol.* **2005**, *7*, 15–22. [[CrossRef](#)]
87. Christensen, K.E.; Mackenzie, R.E. Mitochondrial one-carbon metabolism is adapted to the specific needs of yeast, plants and mammals. *Bioessays* **2006**, *28*, 595–605. [[CrossRef](#)]
88. Blackwell, R.D.; Murray, A.J.; Lea, P.J.; Kendall, A.C.; Hall, N.P.; Turner, J.C.; Wallsgrave, R.M. The value of mutants unable to carry out photorespiration. *Photosynth. Res.* **1988**, *16*, 155–176. [[CrossRef](#)]
89. Timm, S.; Florian, A.; Arrivault, S.; Stitt, M.; Fernie, A.R.; Bauwe, H. Glycine decarboxylase controls photosynthesis and plant growth. *FEBS Lett.* **2012**, *586*, 3692–3697. [[CrossRef](#)]
90. Igamberdiev, A.U.; Bykova, N.V.; Lea, P.J.; Gardestrom, P. The role of photorespiration in redox and energy balance of photosynthetic plant cells: A study with a barley mutant deficient in glycine decarboxylase. *Physiol. Plant.* **2001**, *111*, 427–438. [[CrossRef](#)]
91. Yancey, P.; Clark, M.; Hand, S.; Bowlus, R.; Somero, G. Living with water stress: Evolution of osmolyte systems. *Science* **1982**, *217*, 1214–1222. [[CrossRef](#)]

